

Validation of simulation tools for ultrasonic inspection of austenitic welds in the framework of the MOSAICS project

Souad BANNOUF¹, Déborah ELBAZ¹, Bertrand CHASSIGNOLE², Nicolas LEYMARIE³,
Patrick RECOLIN⁴

¹ EXTENDE, 15 Avenue Emile Baudot, Le Bergson, 91300 MASSY, France, contact@extende.com,
www.extende.com

² EDF R&D, Moret sur Loing, 77818, France, e-mail : bertrand.chassignole@edf.fr

³ CEA, LIST, F-91191, Gif-sur-Yvette cedex, France, e-mail : nicolas.leymarie@cea.fr

⁴ DCNS/CESMAN, La Montagne, 44620, France, e-mail : patrick.recolin@dcnsgroup.com

Abstract

Welded components of nuclear equipment are submitted to volumetric inspection due to regulatory requirements. Because of the polycrystalline structure of the weld, the detection and characterization of defects may be complicated as the ultrasonic beam shows disturbances. Therefore, taking into account complex 3D configurations in modelling codes is a major challenge in order to improve the prediction of the ultrasonic propagation and then to optimize the UT inspections. In this purpose, the MOSAICS project supported by the ANR (French National Research Agency) aims at developing several complementary modelling approaches (finite elements code ATHENA, ray-based models, hybrid model combining the two approaches included in CIVA software) to simulate the propagation of ultrasonic waves in welds. For validation purpose, experimental data have been acquired on representative mock-ups containing calibrated defects. The goal of this paper is to present the comparison between experimental and simulated results obtained in the MOSAICS project.

Keywords: Weld inspection, Anisotropy, Dynamic Ray Tracing, CIVA, ATHENA

1. Introduction

The MOSAICS project, supported by the ANR (French National Research Agency) has started in October 2011 and will finish in January 2015. It includes the following partners: EDF – DCNS (Naval defence) – CEA (French Commission on Atomic Energy) – EXTENDE (CIVA software provider) – Aix-Marseille University – INSA de Lyon (National Institute of Applied Sciences). The goal of the MOSAICS project is to develop modelling codes in order to improve the prediction of the ultrasonic propagation in austenitic welds and to help inspection diagnosis.

So far, studies have been limited to 2D configurations and to one specific welding process (Shield Metal Arc Welding (SMAW)). However, new industrial applications, with increasing complexity in terms of geometry and material (various welding processes) are emerging. As a consequence, complex 3D configurations need to be taken into account in order to understand the wave to microstructure interaction and then to optimize the UT inspection configurations. Finally, the goal is to provide key elements for decisions relating to the integrity of high-risk structures. In the framework of the MOSAICS project, two complementary modelling codes are developed to deal with the problem of ultrasonic testing of austenitic welds exhibiting anisotropic and heterogeneous structures. On the first hand, the 3D finite element (FE) model ATHENA, developed by EDF R&D, allows to study wave propagation in these medias and the beam interaction with complex flaws [1]. On the other hand, in the CIVA software developed by CEA, the beam propagation and defect response are calculated thanks to semi-analytical formulations and dynamic ray tracing model [2-5].

The experimental validation of ATHENA3D and CIVA codes is a second objective of MOSAICS. The goal of this paper is to present the comparison between experimental and simulated results obtained on an industrial application.

2. Modelling codes

2.1 The CIVA dynamic ray tracing model (CIVA_weld)

Various models have been proposed in the literature to simulate the propagation of ultrasonic waves in welds. The CIVA semi-analytical propagation model based on ray theory can be used to this purpose. The weld is described as a set of several anisotropic homogeneous domains with a given crystallographic orientation in each volume. The rays propagate in straight lines in these domains. At each interface, a calculation of the reflected and refracted coefficients is done before calculating the propagation within the next domains. This model is valid provided the domains have dimensions larger than the wavelength and the variations of impedance between two adjacent areas are small.

If these conditions are not fulfilled, a ray based model on a continuously varying description of the grain orientation has to be used. Such models have been developed initially in geophysics [6] and their application to the ultrasonic inspection of austenitic welds is described below.

The dynamic ray tracing model for the propagation in anisotropic and inhomogeneous media has been described by Cerveny [6]. To evaluate ray trajectory, a differential system, called kinematic ray tracing system derived from the Eikonal equation, has to be solved:

$$\frac{dx_i}{dT} = \frac{c_{ijkl}}{\rho} S_l P_j P_k = V_{e_i} \quad (1)$$

$$\frac{dS_i}{dT} = -\frac{1}{2\rho} \frac{\partial c_{ijkl}}{\partial x_i} S_k S_n P_j P_l \quad (2)$$

where T is the travel time along the ray trajectory, c_{ijkl} are the space-dependent components of the elastic stiffness tensor, ρ the density, S_i are the components of the slowness vector, P_i the components of the polarization vector and V_{e_i} stands for the energy velocity components.

These two equations are coupled. The variation of the current ray position with respect to the travel time is expressed by the first equation which explicitly depends on the slowness. Similarly, the second equation defining the variation of the current slowness with respect to the travel time depends on the current position x_i . This system can be solved for compression or shear waves by setting initial conditions according to the considered mode and applying standard numerical techniques such as Euler's method or Runge-Kuttas's method. It allows to obtain curved ray trajectories in media with continuously varying properties.

To solve the system, the elastic constants values and their derivatives at any position inside the weld have to be determined. The latter may be obtained numerically if the weld is described as a grain orientation mapping. This analysis is discussed in section 3.

2.2 The ATHENA code

The ATHENA code is based on solving elastodynamic equation in the calculation zone expressed in terms of stress and velocities of displacements. Associated with a specific Graphic User Interface (GUI), it allows modelling the entire ultrasonic testing chain (specimen, probe, and defect). The particularity of the code relies on the fact that the discretization of the calculation domain uses a Cartesian regular 3D mesh while a separate mesh using the fictitious domains method is used to describe the defect of complex geometry.

This allows combining the rapidity of regular meshes computation with the capability of modelling arbitrary shaped defects. Furthermore, the use of absorbing boundaries (PML = Perfectly Matched Layer) for the calculation zone reduces the size of this area. The last step to reduce the computation time relies on the fact that ATHENA3D has been parallelized and adapted to high-performance computers. However, unlike the 2D version, the current 3D version does not include attenuation model reflecting the phenomenon of scattering at grain boundaries.

Various actions have been conducted to validate the 2D version of the code, especially for the problematic of weld inspection [7-8]. One of the objectives of MOSAICS is to validate and exploit the 3D version of the code [9-10].

3. Weld descriptions

3.1 Macrographs

Different applications involving austenitic stainless steel multipass welds have been identified by the industrial partners (EDF and DCNS). Some of them, corresponding to shielded metal arc welding (SMAW), are illustrated on Figure 1. The EDF application is a 37 mm thick and V-shape weld (Figure 1(a)) realized in vertical-up position. The DCNS application (Figure 1(c)) corresponds to a primary safety valve nozzle weld realized in horizontal-vertical position. Afterwards, this paper focuses on the EDF application.

A Macrograph of the weld associated with the EDF application and obtained in the plane (V'T) is shown on Figure 1(a). Vertical-up welding leads to a grain tilt along the welding direction (WD axis), that was estimated to 18° for this weld (V' axis) (Figure 1(a) right). Because of this disorientation, the incidence plane (VT) is not a symmetry plane of the anisotropic material. Beam deviations out from the incidence plane can potentially occur, the 2D assumption is then no longer valid in simulation.

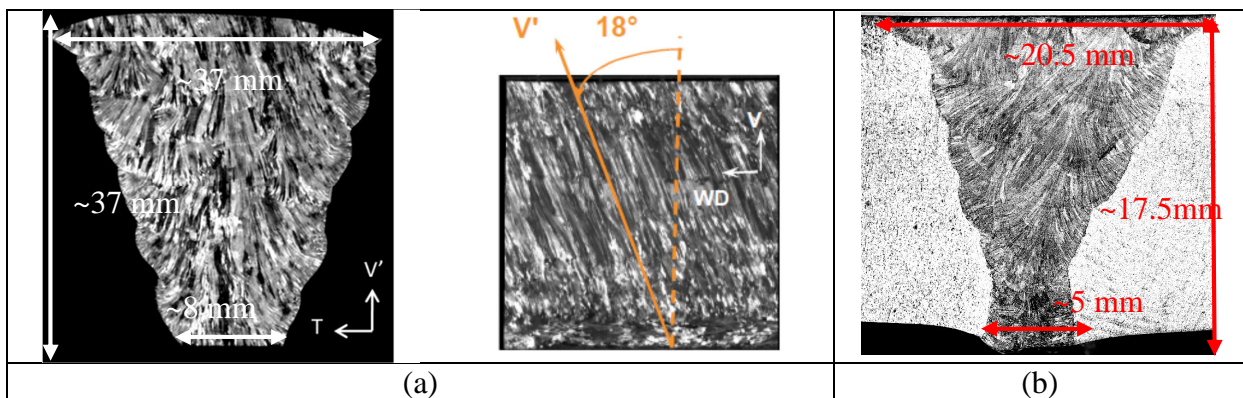


Figure 1: Macrographs of 316L austenitic steel welds. (a) EDF application: V-shape weld in vertical-up position; (b) DCNS application: primary safety valve nozzle in horizontal-vertical position

3.2 Grain orientation mapping

An analysis was performed on this weld macrograph to obtain a grain orientation mapping in a grid made of 2mm side squares which will be used as input data in ATHENA3D. The analysis consisted in applying a Hough transform (method of pattern recognition, in particular straight lines) to the macrograph and measuring the orientations of columnar grains.

The grain orientation values at each point of the weld to be inspected are also required input data to the CIVA model. They have been obtained using a specific plug-in of the ImageJ software developed by the Laboratory of Biomedical Imaging of the Federal Polytechnic School of Lausanne [11]. This plug-in, called OrientationJ, is based on the evaluation of the structure tensor and determines the orientation of every pixel of an image.

Furthermore, to use the dynamic ray tracing model, it is necessary to apply a smoothing filter which width depends on the wavelength λ . The filtering process consists in convolving the image with a Gaussian function characterized by its standard deviation σ . Finally, in order to reduce the loading time of the smoothed mapping, a spatial decimation can be performed.

Figure 2(a) shows the weld map obtained by image processing on ImageJ. Local grain orientations are displayed on this figure. Figure 2(b) corresponds to the same map after smoothing and decimation operations applied in CIVA.

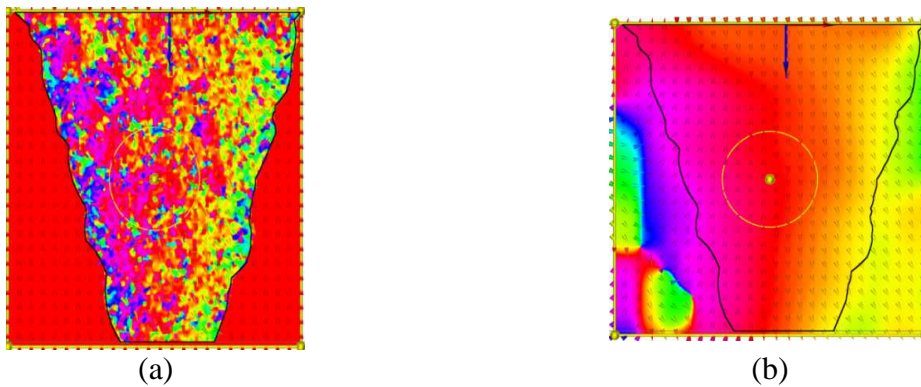


Figure 2: EDF weld maps obtained after image processing of the macrograph (ImageJ software): (a) without smoothing and decimation operations, (b) with smoothing and decimation operations.

3.3 Elastic properties and attenuation coefficients

Elastic properties and attenuation coefficients are other first-order parameters for UT modelling. Elastic constants used in this study are given in Table 1, with the assumption of an orthotropic symmetry. They have been determined from an inverse problem consisting in making use of suitable measurements of ultrasonic velocities [12]. The two sets in Table 1 correspond to measurements on samples machined in two different welds.

Table 1 : Elastic constants for 316L austenitic welds (GPa)

	C_{11}	C_{22}	C_{33}	C_{23}	C_{13}	C_{12}	C_{44}	C_{55}	C_{66}
Set 1	247	247	218	148	148	110	110	110	80
Set 2	250	255	230	137	127	112	102	123	60

The base metal around is assumed to be homogeneous and isotropic. The velocity of longitudinal waves is 5740 m/s while shear waves propagate at 3080 m/s.

The attenuation in the weld at 2.25 MHz is defined by the following coefficients (cf. Table 2) depending on the angle between the propagation direction and the major axis of the columnar grains [13]:

Table 2: Attenuation values in 316L austenitic welds (2.25 MHz frequency)

Angle (°)	0	15	30	45	60	75	90
Attenuation (dB/mm)	0.037	0.036	0.048	0.075	0.115	0.168	0.235

4. Ultrasonic inspection: comparison between experimental and modelling results

4.1 Specimen and inspection description

Ultrasonic inspections were performed on a flat mock-up of 37mm thickness in which five standard defects were machined (see Figure 3):

- 2 Side Drilled Holes (SDH) of 1.5 mm diameter located 25mm under the surface of inspection and on both side of the weld.
- 3 backwall notches of 10 mm high. A notch is located at the center of the weld, while the two others are on both side of the weld. The three notches are respectively separated by 25mm.

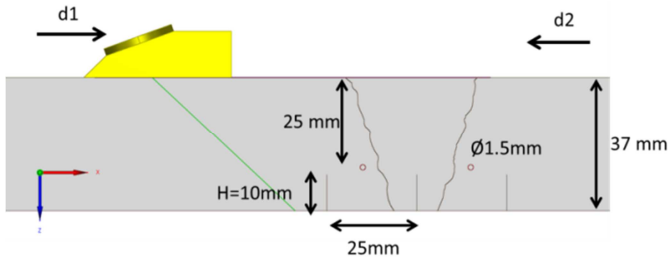


Figure 3: EDF specimen with V shape weld

A 2.25 MHz single-element probe, propagating longitudinal waves at 45° in austenitic steel, was used. The inspections were performed under the two directions d1 and d2 indicated on Figure 3.

4.2 Results

The amplitudes of the different echoes are analysed. The reference amplitude, whatever the scanning direction, corresponds to the amplitude of the flaw located before the weld. Therefore, a negative value stands for an attenuation in the weld.

The variables defining the smoothing filtering and the decimation of the cartography in CIVA dynamic ray tracing module are $\sigma = 4\text{mm}$ and decimation = 3mm. In general, σ is close to the wavelength. In practice, the two variables were chosen in order to minimize the discrepancy between experimental and modelling results in d1 and d2 directions for SDH defects. Once these values are determined, they are used for all simulations on this specimen and whatever the defect being inspected. The influence of these parameters on the amplitude values are discussed in section 5.

Figure 4 shows the Bscans resulting from the SDH inspection along d1 scanning. The SDH amplitudes after weld crossing are reported on Table 3. Simulations were performed with the first set of elastic constants reported on Table 1.

Table 3 : SDH amplitudes after weld crossing

	Experiment (dB)	CIVA (dB)	ATHENA 3D (dB)
Direction d1	-12.7 ± 0.6	-12.3	-9.9

Direction d2	-9.3 ± 0.7	-8.1	-3.8
---------------------	----------------	------	------

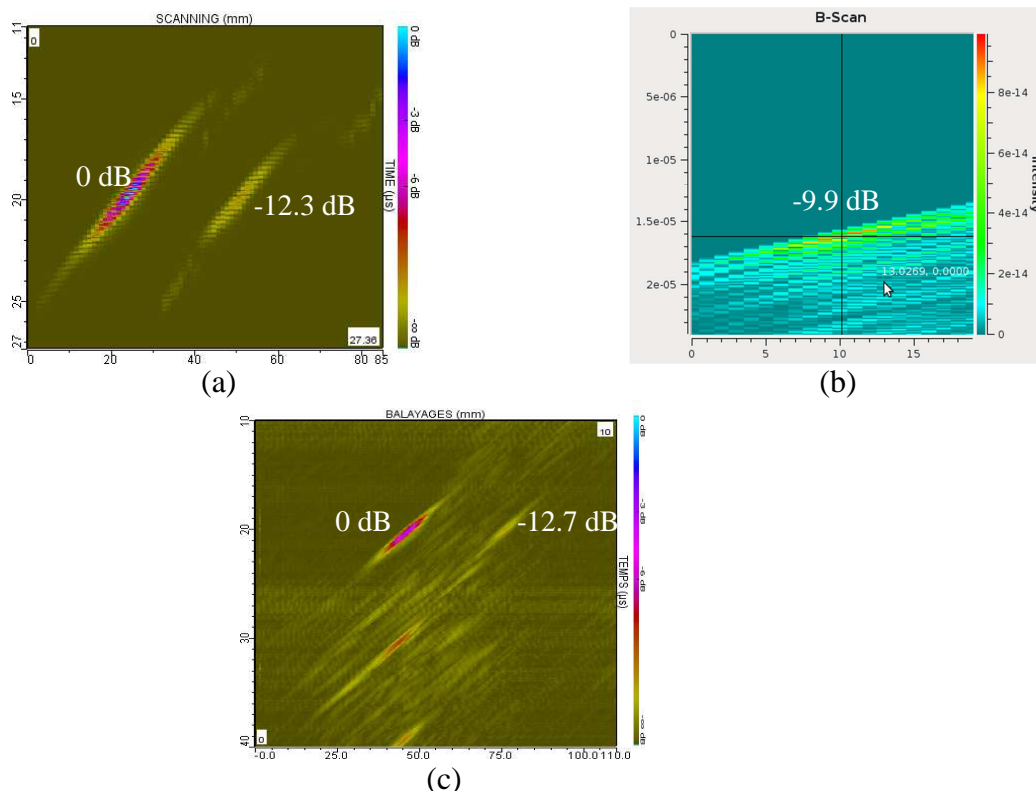
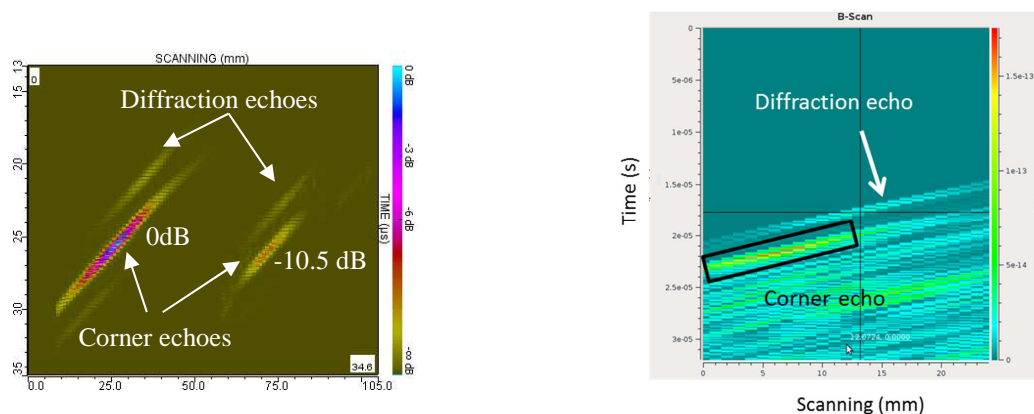


Figure 4: Bscans resulting from the SDH inspection along d1 scanning. (a) CIVA simulated Bscan; (b) ATHENA3D simulated Bscan; (c) Experimental Bscan

Figure 5 shows the Bscans resulting from the notches inspection according d1 scanning. The corner echoes amplitudes after weld crossing and for each scanning direction are reported on Table 4.

Table 4 : Notches corner echoes amplitudes after weld crossing

	Experiment (dB)	CIVA (dB)	ATHENA 3D (dB)
Direction d1	-12.7 ± 0.6	-10.5	-7.9
Direction d2	-10.6 ± 0.9	-6.3	-5.9



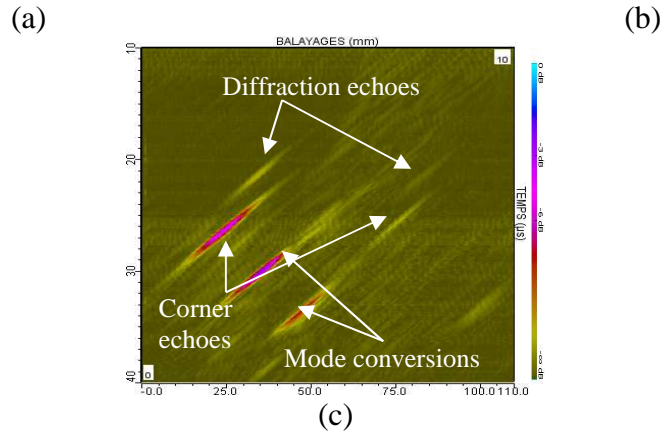


Figure 5: Bscans resulting from the notch inspection along d1 scanning. (a) CIVA simulated Bscan; (b) ATHENA3D simulated Bscan, (c) experimental Bscan

Both codes reproduce the attenuation effects in the weld due to beam division and wave scattering in the anisotropic and heterogeneous coarse grain structure.

CIVA results, taking into account attenuation coefficients and with optimized σ and decimation parameters, are in good agreement with experimental ones. These preliminary results seem to validate the dynamic ray tracing CIVA module but additional tests are necessary to conclude.

The current version of ATHENA3D code partially predicts the weld attenuation. Indeed, scattering is only generated at the homogeneous anisotropic domains interfaces on the weld grid description. The implementation of an attenuation model is ongoing and will be based on the characterization work carried out at INSA Lyon [14]. The simulations will be repeated by the end of the project. Furthermore, a structural noise due to backscattering is visible on experimental Bscans (Signal-to-Noise Ratio (SNR) close to 10 dB for the corner and the SDH echoes). This effect has not been simulated with the CIVA version used in this study. Regarding ATHENA, backscattering is produced by the weld grid description but its level is overestimated. To obtain the “clean” Bscans presented on Figures 4 and 5, the simulation without defect has been subtracted to the simulation with defect.

This discussion clearly shows that further investigations are necessary to optimize the weld description and determine its impact on the modelling results. First results are presented on the next section to address this issue.

5. Modelling influential parameters

5.1 CIVA influential parameters

As explained in section 2.2, the CIVA_weld module needs to specify 2 variables: the size of the Gaussian window used as smoothing filter (σ) and the decimation parameter.

As the definition of these parameters remains currently empirical, the sensitivity of SDH echoes to those 2 parameters was studied. Figure 6 presents the results obtained from this study. The curves correspond to the SDH echoes amplitude after the waves have passed through the weld according to d1 or d2 scanning direction (Figure 6 (a) and (b) respectively). These results show that whatever the decimation value and the scanning direction, the SDH echoes amplitude converges when σ value increases. However, this amplitude is not the one measured experimentally and the curve evolution changes according the direction studied. Furthermore, for lower values of σ , the simulated amplitudes may be very different from one value to the other. This shows the high sensitivity of the results with these parameters. It

would be advisable to set these parameters automatically with a theoretical justification based on the propagation analysis of the coherent wave in a polycrystalline material.

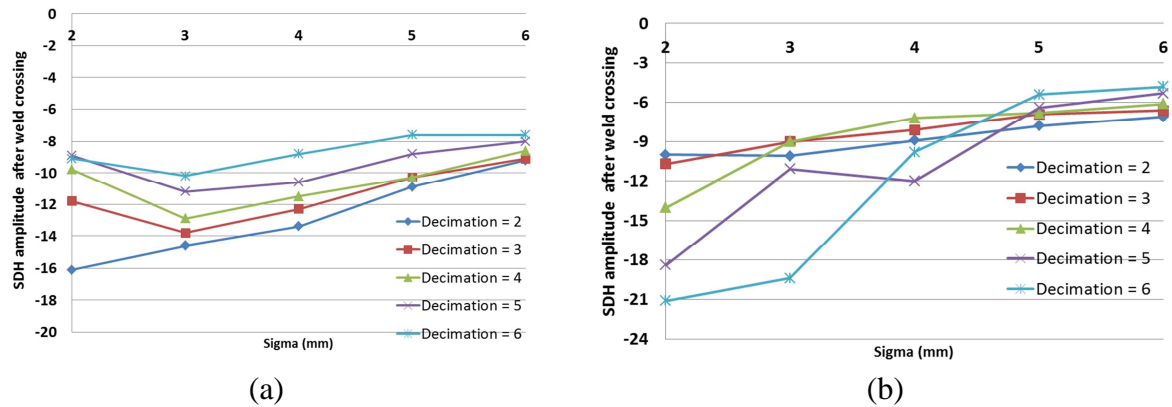


Figure 6: Evolution of the SDH echoes amplitude after weld crossing (a) after d1 inspection; (b) after d2 inspection

5.2 ATHENA3D influential parameters

5.2.1 Influence of the weld grid description

The weld description, or more precisely the size and shape of the anisotropic and homogeneous domains describing the heterogeneous structure, is a key parameter for the UT modelling with ATHENA. The description used in section 4.2 was a grid made of squares of 2mm side (description 1). In order to study the influence of this parameter, two additional descriptions were modelled: a grid made of squares of 1mm side (description 2) and a higher scale description with a limited number of domains merging the square domains with similar orientations (description 3). For this latter, the information on the gradual variation of grain orientation is lost but the boundaries between two domains are more closely related to the reality. It was in particular demonstrated in previous studies that description 3 predicted right echo amplitudes with the 2D version of ATHENA taking into account a model for scattering attenuation [8].

The amplitude of the SDH echo after weld crossing according to d1 direction and for these three descriptions are reported on the Table 5. Structural noise level and signal to noise ratio (SNR) are also indicated.

Table 5: Influence of weld description: Comparison of SDH amplitude after weld crossing according to d1 direction

	Experiment	Description 1 (2 mm grid)	Description 2 (1 mm grid)	Description 3
Defect echo amplitude (dB)	-12.5	-11.0	-7.0	-3.5
Structural Noise amplitude (dB)	-23.0	-11.0	-12.0	-18.0
SNR (dB)	11.5	0.0	5.0	14.5

Changing the grid size from 2mm to 1mm leads to smooth the grain structure and then clearly decreases the attenuation due to scattering on boundaries between square domains. On the other hand, the noise level is similar and far higher than the experimental value. As expected, the defect echo amplitude is overestimated with description 3 as the number of interfaces was

significantly decreased. As a result, the simulated noise level is also decreased and closer than the experimental one.

This preliminary study confirms the significant influence of the weld description on the FE modelling results in terms of echo amplitudes and noise level. As mentioned previously, future works will address the implementation of an attenuation model in ATHENA3D that will have an impact both on defect and noise echoes. Then, new calculations will be performed to give recommendations on suitable weld descriptions depending on the phenomenon studied. Moreover, another approach consists in applying grain-scale modelling [16] but this approach is currently limited to small calculation zone with a 3D FE code.

5.2.2 Influence of the C_{ij} elastic constants

The anisotropic matrix coefficients C_{ij} are other parameters that may influence the results. They describe the anisotropy degree of the weld but they are difficult to measure accurately. Therefore, the influence of small changes in the C_{ij} coefficients has been evaluated. With this aim in view, ATHENA3D calculations were performed with the second set of elastic constants of Table 1 and the results were compared to the previous ones. A 2mm-square grid was used for the weld meshing.

Table 6 : SDH echo amplitude and Signal to Noise ratio for two sets of elastic constants

D1	C_{ij1}	C_{ij2}
Amplitude (dB)	-11.0	-8.5
SNR (dB)	0.0	4.0

The results obtained on the SDH inspected along d1 are reported on Table 6. For this specific configuration, they highlight an influence of the C_{ij} coefficients. Indeed, contrary to the first set of the C_{ij} coefficients, C_{ij2} values describe a less anisotropic tensor, the SNR is increased of 4 dB.

In conclusion, these results show the sensitivity of the CIVA and ATHENA3D codes to the weld description. This complex problem is not yet resolved and extending studies are under investigations [15].

6. Conclusion

The MOSAICS project goal is to develop modelling codes in order to predict ultrasonic propagation in austenitic welds and then to optimize the UT inspection of this complex materials. This paper gives an overview of the first results of the ATHENA3D code and a new dynamic ray tracing model in inhomogeneous anisotropic media developed in CIVA).

The new CIVA module integrating a continuous varying description of a highly heterogeneous weld significantly improves the predication of the beam propagation and the echo amplitudes. However, the adjustment of parameters used in the filtering process to obtain the weld description needs to be examined in more details.

3D finite element modelling is now available with ATHENA code and allows removing the limitations of the previous 2D version in terms of material, probe characteristics or defect morphology. Regarding austenitic weld inspection, further investigations are necessary to implement an attenuation model in the code and to better understand the influence of the material input data (scale of weld description, elastic constants values) on the results.

For this goal, these preliminary results should be completed by additional studies on other types of welds (for example the DCNS application for the primary safety valve nozzle on Figure 1(b)) and others propagation modes (LW60°).

Acknowledgements

This work was realized in the framework of the MOSAICS project (Modelling of an austenitic stainless steel weld inspected by ultrasonic technics) which is supported by the French National Agency of Research.

References

1. E. Becache et al., An analysis of new mixed finite elements for the approximation of wave propagation problems, *SIAM J Numer Anal* 37 (2000) 1053-84.
2. P. Calmon et al., CIVA: an expertise platform for simulation and processing NDT data, *Ultrasonics* 44 (2006) 975-979.
3. N. Leymarie et al., 'Modeling of weld inspection by using a paraxial ray-tracing approach in a variable anisotropy medium', BINDT congress, July 2013.
4. K. Jezzine et al, 'Evaluation of ray-based methods for the simulation of UT welds inspection', 39th Review of Progress in QNDE', Vol 32B, pp 1073-1080, 2013.
5. A. Gardahaut, Développements d'outils de modélisation pour la propagation ultrasonore dans les soudures bimétalliques, Thèse de doctorat, Université Paris Diderot – Paris 7, 2013.
6. V. Cerveny, *Seismic Ray Theory*, Cambridge University Press, Cambridge, 2001.
7. B. Chassignole et al., 'Modelling the attenuation in the ATHENA finite elements code for the ultrasonic testing of austenitic stainless steel welds', *Ultrasonics*, vol. 49, pp. 653-658, 2009.
8. B. Chassignole, et al, Ultrasonic examination of a CVCS weld, *Proceedings of 6th ICNDE*, Budapest, 2007.
9. C. Rose et al., 'ATHENA 3D: A finite element code for ultrasonic wave propagation, 12th Anglo-French Physical Acoustics Conference (AFPAC2013) IOP Publishing, *Journal of Physics: Conference Series* 498 (2014) 012009
10. B. Chassignole et al, 3D modelling of ultrasonic testing in austenitic welds, BINDT conference, July 2013.
11. ImageJ : Image Processing and Analysis in Java
12. Chassignole et al, Characterization of austenitic steel welds for ultrasonic NDT, *Review of Progress in QNDE*, vol 19B, 1325-1332, (2000)
13. M.-A. Ploix et al., Measurement of ultrasonic scattering attenuation in austenitic stainless steel welds: Realistic input data for NDT numerical modelling, *Ultrasonics* (2014), in press, <http://dx.doi.org/10.1016/j.ultras.2014.04.005>
14. N. Alaoui-Ismaili, P. Guy, B. Chassignole, Experimental determination of the complex stiffness tensor and Euler angles in anisotropic media using ultrasonic waves, in: *AIP Conference Proceedings*, AIP Publishing, 2014: pp. 934–940.
15. F. Rupin et al, Probabilistic approaches to compute uncertainty intervals and sensitivity factors of ultrasonic simulations of a weld inspection, *Ultrasonics*, vol. 54, Issue 4, pp. 1037-1046
16. P.E. Lhuillier et al, Overview of the recent developments on grain-scale modeling to simulate ultrasonic scattering with a 2D finite element code, *ICNDE* 2013.